Palaeogeography, Palaeoclimatology, Palaeoecology 572 (2021) 110409

Contents lists available at ScienceDirect

Palaeogeography, Palaeoclimatology, Palaeoecology

journal homepage: www.elsevier.com/locate/palaeo

Keratose sponge–microbial consortia in stromatolite-like columns and thrombolite-like mounds of the Lower Ordovician (Tremadocian) Mungok Formation, Yeongwol, Korea

Duy Pham [a], Jongsun Hong [b], Jeong-Hyun Lee [a,c,*]

[a] Department of Astronomy, Space Science, and Geology, Chungnam National University, Daejeon 34134, Republic of Korea
[b] Department of Geology, Kangwon National University, Chuncheon 24341, Republic of Korea
[c] Department of Geological Sciences, Chungnam National University, Daejeon 34134, Republic of Korea

ARTICLE INFO

Editor: Isabel Montanez

Keywords:
Keratolite
Sponge-microbial reef
Laminar reef
Cluster reef
Great Ordovician Biodiversification Event

ABSTRACT

Lower Ordovician stromatolite-like columns and thrombolite-like mounds, composed of fossilised keratose sponges (keratolites) and microbial carbonates, are reported from the Tremadocian Mungok Formation, Yeongwol, Korea. The stromatolite-like columns, which are up to 10 cm wide and high, consist of an inner core with low-angled (10–45°) layers that are covered by high-angled (>45°) layers. The inner core is made up of millimetric layers of alternating keratolite and microbial carbonate, and microbial carbonate dominantly comprises the outer cover. The entire columns are surrounded by bioclastic packstone to grainstone. The thrombolite-like mounds are domes a maximum of 100 cm high and 40–60 cm wide embedded within lime mud and shale. These mounds consist of keratolite–microbial carbonate clots and minor lithistid sponge–microbial carbonate clots. The stromatolite-like columns were formed in a high-energy subtidal setting, in which laminoid keratolite and microbial carbonate formed the tight laminar frame columns. Continued growth of the column narrowed the intercolumnar space, resulting in higher-energy hydrodynamic conditions that limited the growth of sponges but promoted growth of microbial organisms. In contrast, thrombolite-like mounds developed in a low-energy environment below fair-weather wave base, where irregular to bulbose keratose sponges with minor lithistid sponge–microstromatolite associations formed cluster reefs. There appear to have been ecological and/or environmental factors that affected the distribution of these sponges; keratose and lithistid sponges rarely occur together in the Mungok reefs, whereas lithistids are pervasive within coeval intermediate-energy microbial reefs elsewhere. These results demonstrate the importance of hydrodynamic controls on overall reef morphology and configurations during the Early Ordovician, and suggest that keratosan–microbial consortia may have been an integral component of the Great Ordovician Biodiversification Event, together with the lithistid sponge–microbial consortium.

1. Introduction

Sponge–microbial consortia are regarded as having been a critical reefal association throughout the Phanerozoic (Brunton and Dixon, 1994). They were especially important during the early stage of metazoan evolution in the early Palaeozoic (Lee and Riding, 2018). Archaeocyath sponges were the first metazoans that globally flourished and constructed reefs together with microbes in the early Cambrian (late Terreneuvian to Epoch 2) (Rowland and Shapiro, 2002; Gandin and Debrenne, 2010; Pruss et al., 2012; Zhuravlev et al., 2015; Cordie et al., 2019). Archaeocyath–microbial reefs disappeared in the late early Cambrian (Age 4 of Epoch 2), and lithistid sponge–microbial reefs flourished during the mid–late Cambrian (Miaolingian–Furongian) and diversified in the Early Ordovician (Lee et al., 2016a; Lee and Riding, 2018). Through the Ordovician Period, the lithistid–microbial reefs were gradually augmented and replaced by newly appearing skeletal reef builders, including calathiids, pulchrilaminids, stromatoporoids, tabulate and rugose corals, bryozoans, receptaculitids, and other groups (Webby, 2002; Adachi et al., 2011; Kröger et al., 2017; Lee and Riding, 2018; Elias et al., 2021). The newly appeared skeletal reefs with stromatoporoid sponges dominated reef ecosystems since the Middle Ordovician (late Darriwilian) and persisted until the Late Devonian

* Corresponding author at: Department of Astronomy, Space Science, and Geology, Chungnam National University, Daejeon 34134, Republic of Korea
E-mail addresses: phduy.geo@gmail.com (D. Pham), jhong@kangwon.ac.kr (J. Hong), jeonghyunlee@cnu.ac.kr (J.-H. Lee).

https://doi.org/10.1016/j.palaeo.2021.110409
Received 7 February 2021; Received in revised form 29 March 2021; Accepted 11 April 2021
Available online 17 April 2021

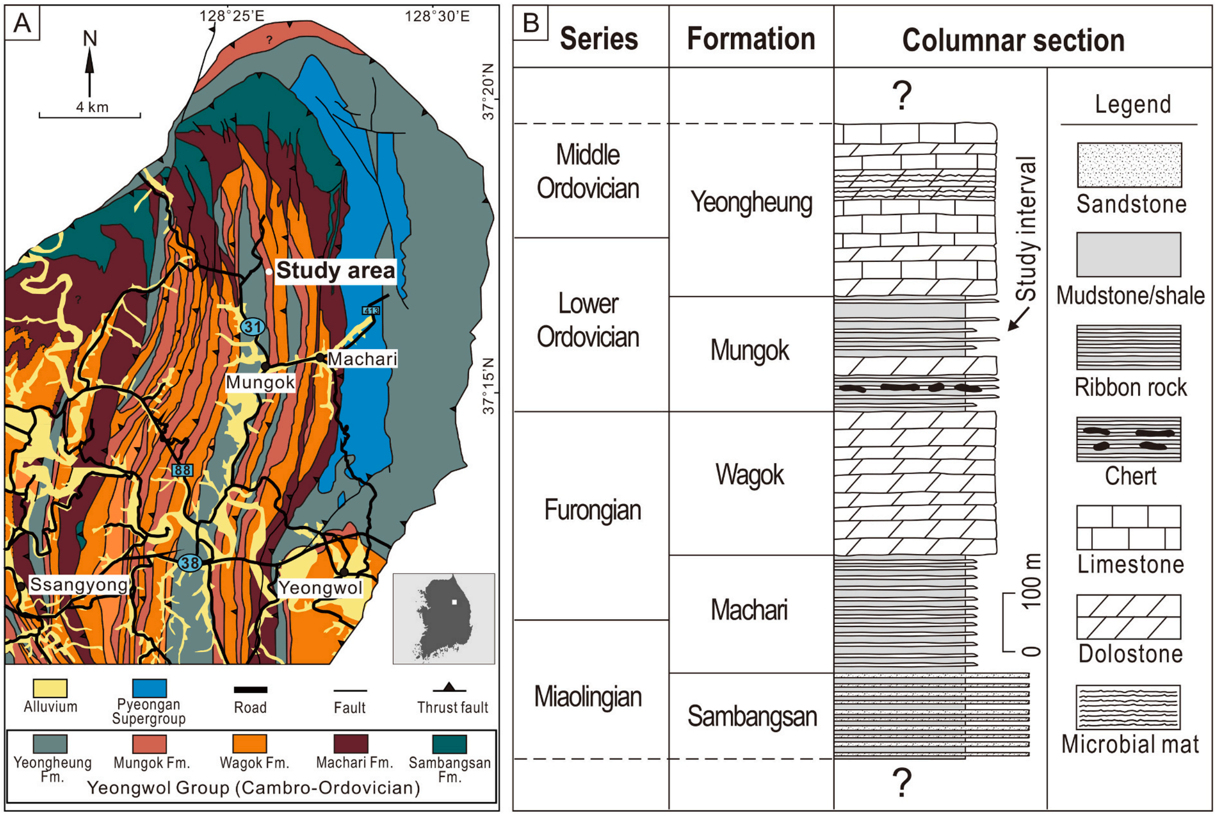

Fig. 1. Geological setting of the study area. (A) Geological map of the Yeongwol Group (modified after Lee, 1995). The location of the study area (the Araetgol section) is marked by a white dot (37°17′07"N, 128°25′58″E). (B) Schematic stratigraphic column of the Yeongwol Group (after Lee, 2020a).

mass-extinction event. These stromatoporoid reefs are the most typical Palaeozoic reef type (Copper, 2011; Kershaw, 2015; Kershaw et al., 2018).

Keratose sponges, a group of demosponges that lack spicules but possess a skeleton of spongin fibres, have recently been recognised as an important contributor to reefs throughout the Phanerozoic (Luo and Reitner, 2014). The term 'keratolite' has been suggested to denote fossilised keratosan carbonates that are often associated with microbial carbonates and formed reefs (Lee and Riding, 2021b). Keratolites are often described as vermiform fabrics (sensu Walter, 1972) within microbialites. Previously reported examples of laminated keratolite–microbial carbonate constructions often superficially resemble classic stromatolites, and are frequently difficult to distinguish from stromatolites in the field (Luo and Reitner, 2016; Lee and Riding, 2021b and references therein). Many keratolite–stromatolite assemblages were previously regarded as microbialites devoid of skeletal organisms, and their true distribution in the geological record would thus have been underestimated (e.g., Lee et al., 2014; Luo and Reitner, 2014, 2016; Luo, 2015; Lee and Riding, 2021b).

Keratolite–microbialite associations are commonly found in early Palaeozoic reefs (Lee and Riding, 2021b), and could have been an integral component of the early Palaeozoic biodiversification events—the Cambrian Explosion and the Great Ordovician Biodiversification Event (GOBE) (Lee et al., 2015). In this study, we describe two different types of bioherms from the Lower Ordovician Mungok Formation, Yeongwol, Korea, that superficially resemble stromatolites and thrombolites, which were mainly constructed by keratose sponge–microbial consortia in addition to minor lithistid sponges. The aim of this study is to determine the reef-building roles of keratose sponge–microbial associations in these two different types of bioherm, and to discuss the factors controlling Early Ordovician reef ecosystems together with the better-known lithistid sponge–microbial associations. The results of this study will help to elucidate how the keratosan–microbial consortium contributed to reef ecosystems during the incipient stage of the GOBE.

2. Geological setting and methods

The Taebaeksan Basin, located in the central–eastern part of the Korean Peninsula (Fig. 1A), contains the lower Palaeozoic Joseon Supergroup that consists of the Taebaek, Yeongwol, Yongtan, Pyeongchang, and Mungyeong groups (Choi and Chough, 2005). The Yeongwol Group contains the Sambangsan, Machari, Wagok, Mungok, and Yeongheung formations in stratigraphic ascending order. The Sambangsan, Machari, and Wagok formations are Cambrian in age; the Mungok and Yeongheung formations are Ordovician in age (Kobayashi, 1966; Choi, 1998) (Fig. 1B). The palaeogeographic location of the Yeongwol Group is problematic. The Sino-Korean Block (to which most of the Joseon Supergroup belongs) and the South China Block, both of which were microcontinents located at the margin of Gondwana during the early Palaeozoic, collided in the late Permian–Triassic and became eastern Asia (Cluzel et al., 1991; Chough et al., 2000; Chough, 2013; Zhao et al., 2021). The Yeongwol Group may have been located in the outer part of the Sino-Korean Block (Kwon, 2012; Choi, 2019) or in the South China Block (Cluzel et al., 1991), and became juxtaposed with the rest of the Joseon Supergroup during the collisional event (Chough, 2013).

The Mungok Formation is Early Ordovician (Tremadocian) in age (Lee, 2020b) based on the identification of three trilobite biozones (the *Yosimuraspis*, *Kainella*, and *Shumardia* zones) (Kim and Choi, 2000) and five graptolite biozones (the *Anisograptus matanensis*, *Adelograptus* cf. *tenellus*, *Callograptus* spp., *Paradelograptus antiquus*, and *Aorograptus victoriae* zones) (Cho and Kim, 2007) (Fig. 2). This succession, which is approximately 200 m thick, mainly consists of ribbon rock (alternating thin beds of lime mudstone and shale), packstone to grainstone, limestone conglomerate, and marlstone to shale facies, and is interpreted as subtidal ramp deposits (Kim and Choi, 2000; Choi et al., 2001; Kim et al.,

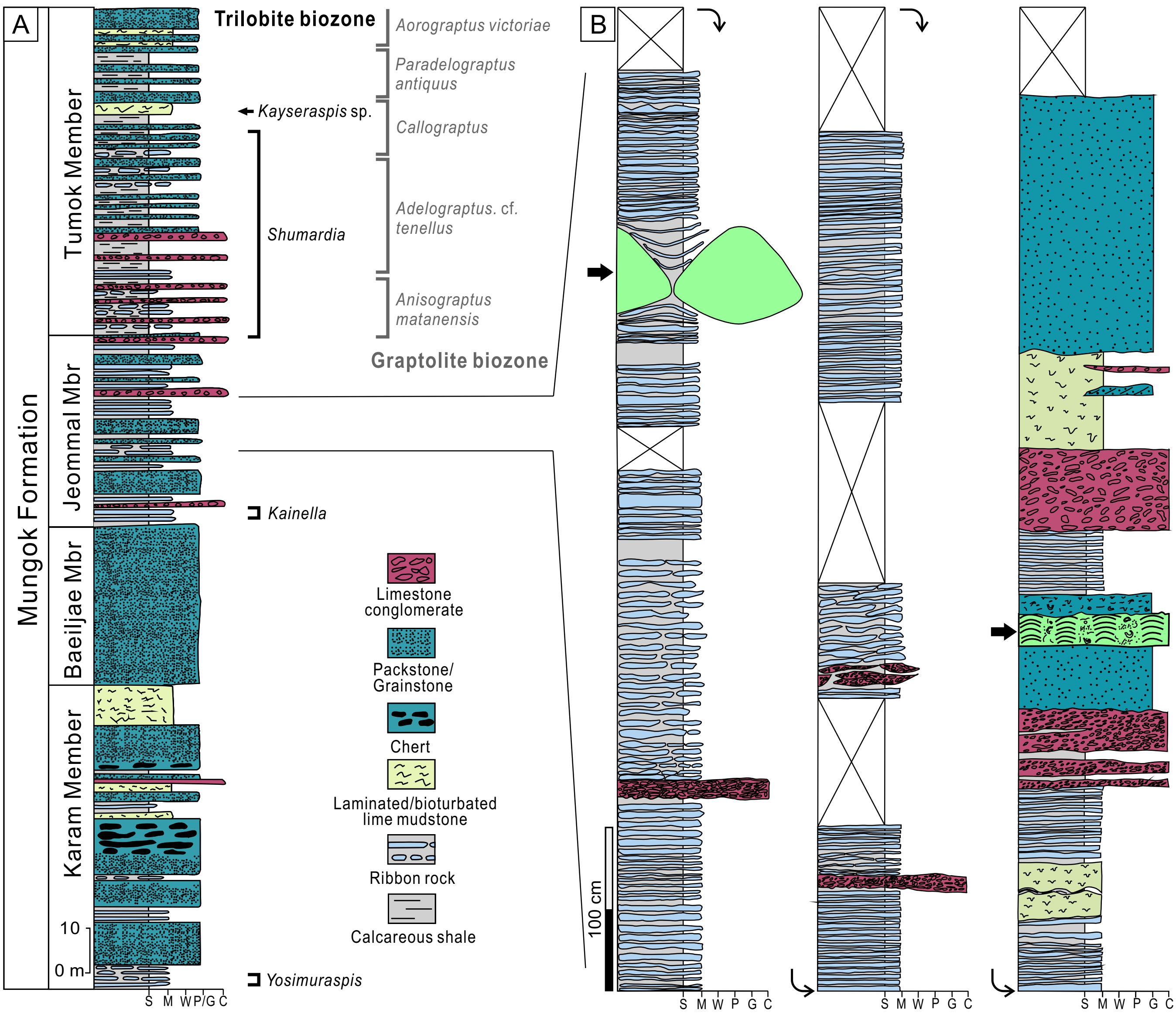

Fig. 2. (A) Generalised stratigraphic log of the Mungok Formation (after Kim et al., 2014). Trilobite biozones after Kim and Choi (2000) and Lee (2020b). Conodont biozones after Cho and Kim (2007). (B) Detailed stratigraphic log of the Araetgol section, which exposes the middle part of the Jeommal Member of the Mungok Formation. The arrows indicate the stratigraphic horizons of the columnar stromatolite-like and thrombolite-like mounds. Abbreviations: S = shale, M = mudstone, W = wackestone, P = packstone, G = grainstone, C = conglomerate.

2014). The formation is further subdivided into four lithostratigraphic units: the Karam, Baeiljae, Jeommal, and Tumok members in stratigraphic ascending order (Kim and Choi, 2000) (Fig. 2A). The Karam Member consists of ribbon rock and packstone to grainstone with minor chert nodules. The overlying Baeiljae Member is characterised by massive dolostone with locally preserved packstone to grainstone texture. The Jeommal and Tumok members mainly consist of ribbon rock and limestone conglomerate, with additional marlstone in the Tumok Member (Kim et al., 2014). Occurrence of the *Anisograptus matanensis* graptolite biozone in the basal Tumok Member (Fig. 2A) suggests a lower Tremadocian age for the Karam, Baeiljae and Jeommal members (Cho and Kim, 2007; Goldman et al., 2020).

The studied samples were collected from the middle Jeommal Member in the Araetgol section, located ~10 km northwest of Yeongwol city (Fig. 1A). The section exposes a ~25-m-thick succession of the Baeiljae to Jeommal members. A 15-m-thick bioherm-bearing succession in the Jeommal Member was measured at 1:10 scale (Fig. 2B). Complementary samples were collected for microfacies analysis at vertical spacings of less than 20 cm. To describe the bioherms, 24 polished slabs and more than 400 large-format thin sections (7.6 × 5.2 cm) cut perpendicular to the bedding were prepared.

3. Results

3.1. Components of the Mungok bioherms

Two types of bioherms were recognised in outcrop on the basis of their different macro- and mesostructures: columnar stromatolite-like (Fig. 3A, B) and domal thrombolite-like bioherms (Fig. 3C). The main constituents of these bioherms are keratolites and microbial carbonates. Minor components include lithistid sponges, various bioclasts (bivalves, crinoids, trilobites, gastropods, and cephalopods), and intraclasts, as well as a considerable amount of secondary sparry cement and dolomite.

3.1.1. Keratolite

The keratolite (sensu Lee and Riding, 2021b), which comprises

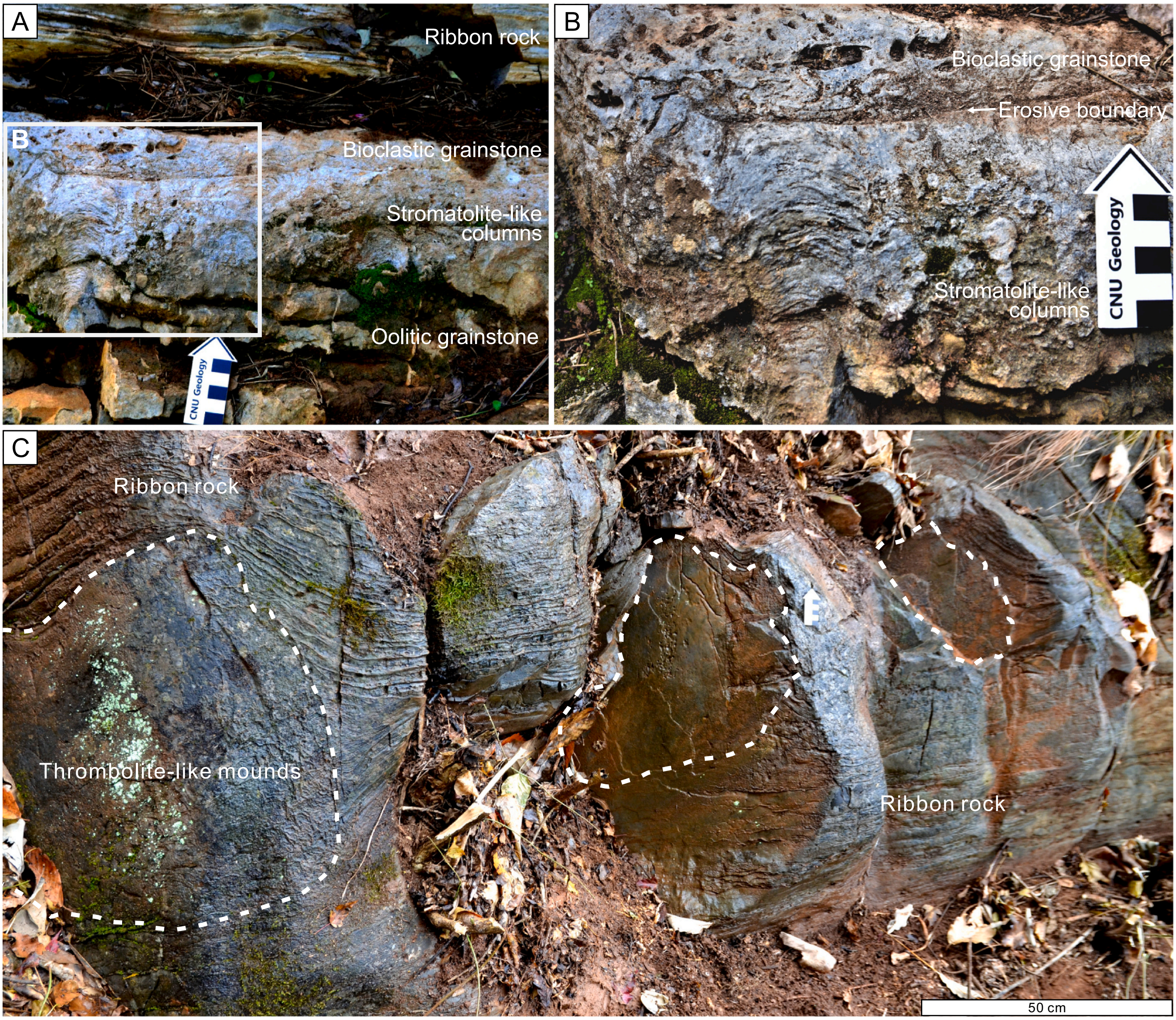

Fig. 3. Outcrop photographs of the stromatolite-like columns and thrombolite-like mounds at the Araetgol section. (A) Outcrop view of stromatolite-like columns. Scale in centimetres. (B) Close-up view of (A). Note occurrence of a sharp erosive boundary above the stromatolite-like column. Scale in centimetres. (C) Outcrop view of the thrombolite-like mounds.

calcified remains of keratose sponges (Luo and Reitner, 2014, 2016), is characterised by a fibrous network of irregular branching sparry filaments that are embedded within micrite (Fig. 4). The filaments are up to a few millimetres long and less than 100 μm wide, with a generally constant diameter (Fig. 4C, D). The outlines of keratolite bodies are often diffuse. The keratolites often laterally grade from dense to loose networks (Fig. 4B, C), and gradually change upward into peloids that are in turn overlain by blocky calcite cement (Fig. 4D), possibly implying early degradation of sponges (Lee et al., 2016b). Bioclasts, which are rarely found within the network (Fig. 4D), would have been trapped in the fibrous networks of the keratosans (Lee and Riding, 2021a).

3.1.2. *Microbial carbonate*

The microbial carbonate is characterised by flat to wavy laminated and non-laminated structures devoid of calcimicrobes. The laminated microbial carbonate forms layers a few millimetres thick (Fig. 5C) or vertically stacked domal, irregular, columnar, to branched micro-stromatolites a maximum of 10 mm high and 8 mm wide (Fig. 5D). The former type is pervasive in the stromatolite-like columns, whereas the latter occurs only in the thrombolite-like mounds. The laminated microbial carbonate is composed of laterally discontinuous, repeated alternations of lighter grey peloidal micritic and darker grey homogeneous micritic laminae less than 100 μm thick. The non-laminated microbial carbonate forms millimetre-scale patches, and occurs in the thrombolite-like mounds. These carbonate patches are composed mainly of darker micritic lumps, with or without subordinate bunches of peloidal micrite. The micritic lumps, <1 mm in size, are bulbous, lobate to irregular forms, and commonly coalesced vertically and laterally.

The laminated microbial carbonate would have formed by lithification of microbial mats (Keupp et al., 1993; Arp et al., 2001; Riding, 2011). Micritic to microclotted fabrics of microbial carbonates represent calcification of the extracellular polymeric substances of sulphate-reducing bacteria (Riding, 2011). Very thin microbial layers are similar to the "filmy structure" of Precambrian stromatolites (Bertrand-Sarfati, 1976; Knoll and Semikhatov, 1998), and would have resulted

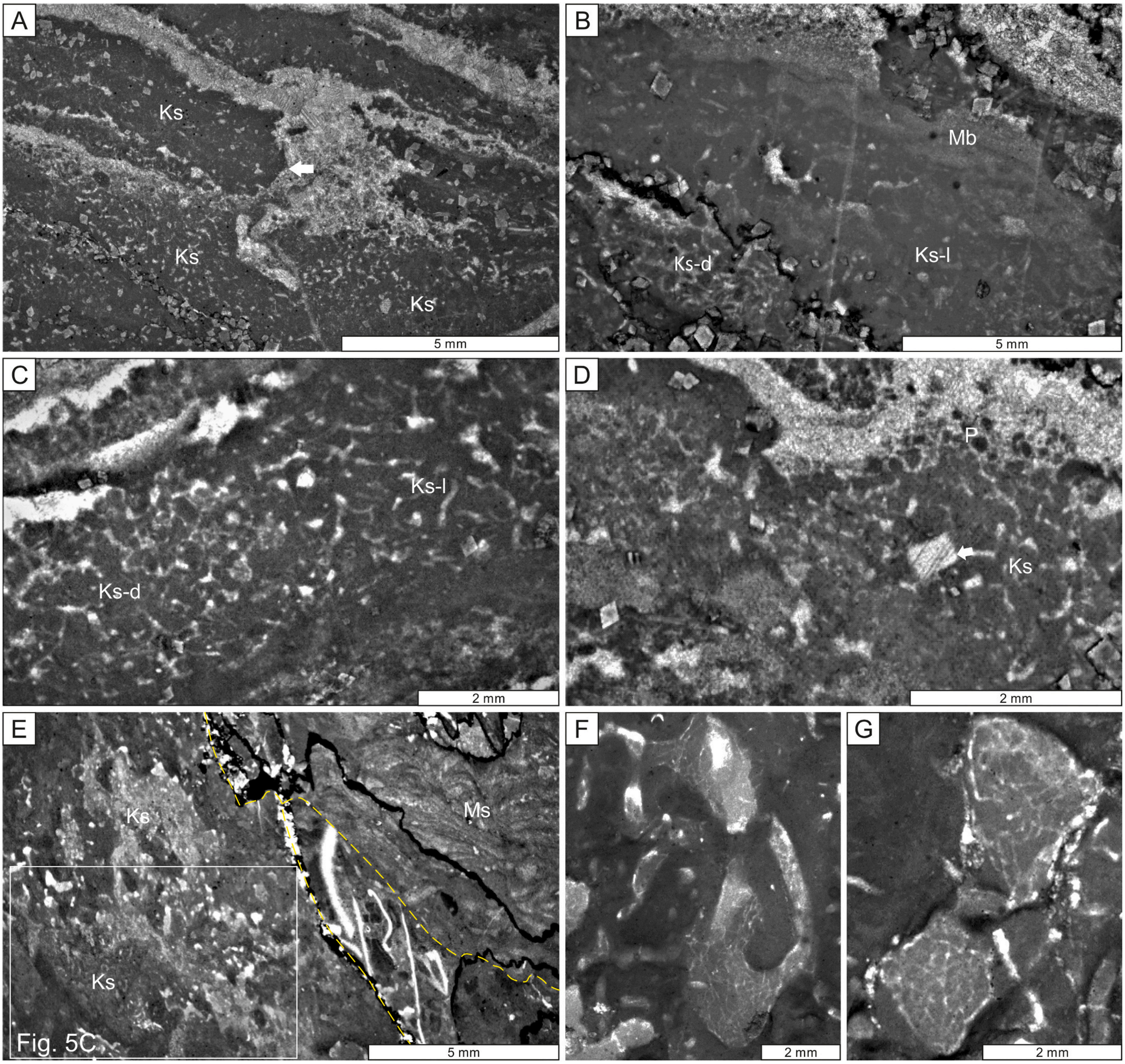

Fig. 4. Photomicrographs of the keratolite. (A–D) Keratolites in the stromatolite-like columns. (A) Keratolite (Ks) layers separated by blocky calcite cement layers. Post depositional calcite cement vertically cuts the keratolite layer (arrow). (B) Dense (Ks-d) and loose (Ks-l) keratolite networks overlain by a crudely laminated microbial carbonate layer (Mb). (C) Lateral gradational change from a dense to loose keratolite network. (D) Keratolite grading upward into peloids (P) and sparry calcite. Note the occurrence of a crinoid fragment in the keratolite (arrow). (E–G) Keratolites in the thrombolite-like mounds. (E) Keratolite surrounded by bioclastic/intraclastic packstone (dashed line) via stylolites, and in turn overlain by microstromatolites (Ms). (F, G) Well-preserved keratolite patches.

from the primary growth of microbial organisms (Harwood and Sumner, 2012).

3.1.3. Other components

Lithistid sponges are one of the most common components in the intercolumnar sediments, but are also locally found in thrombolite-like bioherms. These sponges are characterised by well- to poorly preserved cylindrical to conical shapes, and are generally 10–20 mm (maximum 32 mm) in diameter (Fig. 6). Their walls contain ladder-like trabs with abundant canals (Fig. 6C, D). Altogether, these characteristics suggest that these lithistid sponges belong to Family Anthaspidellidae, and some to the genus *Archaeoscyphia* judging by the occurrence of wings (Fig. 6B) (Rigby and Desrochers, 1995; Church, 2017).

Other biogenic components include bioclasts such as trilobites, bivalves, gastropods, crinoids, and cephalopods (Fig. 7A, B). These bioclasts mostly form bioclastic wackestone to packstone between the bioherms or occur in the bioclastic grainstone that sharply truncates the stromatolite-like columns. Bioclasts were also rarely observed within the bioherms. Micritic intraclasts, a common component of lower Palaeozoic successions (Wright and Cherns, 2016), are found in the intercolumnar/interbioherm spaces (Fig. 7C).

Two important abiotic components, blocky calcite cement and coarse dolomite crystals, occur in the bioherms. The blocky calcite is common within the stromatolite-like columns. The calcite cement is often parallel

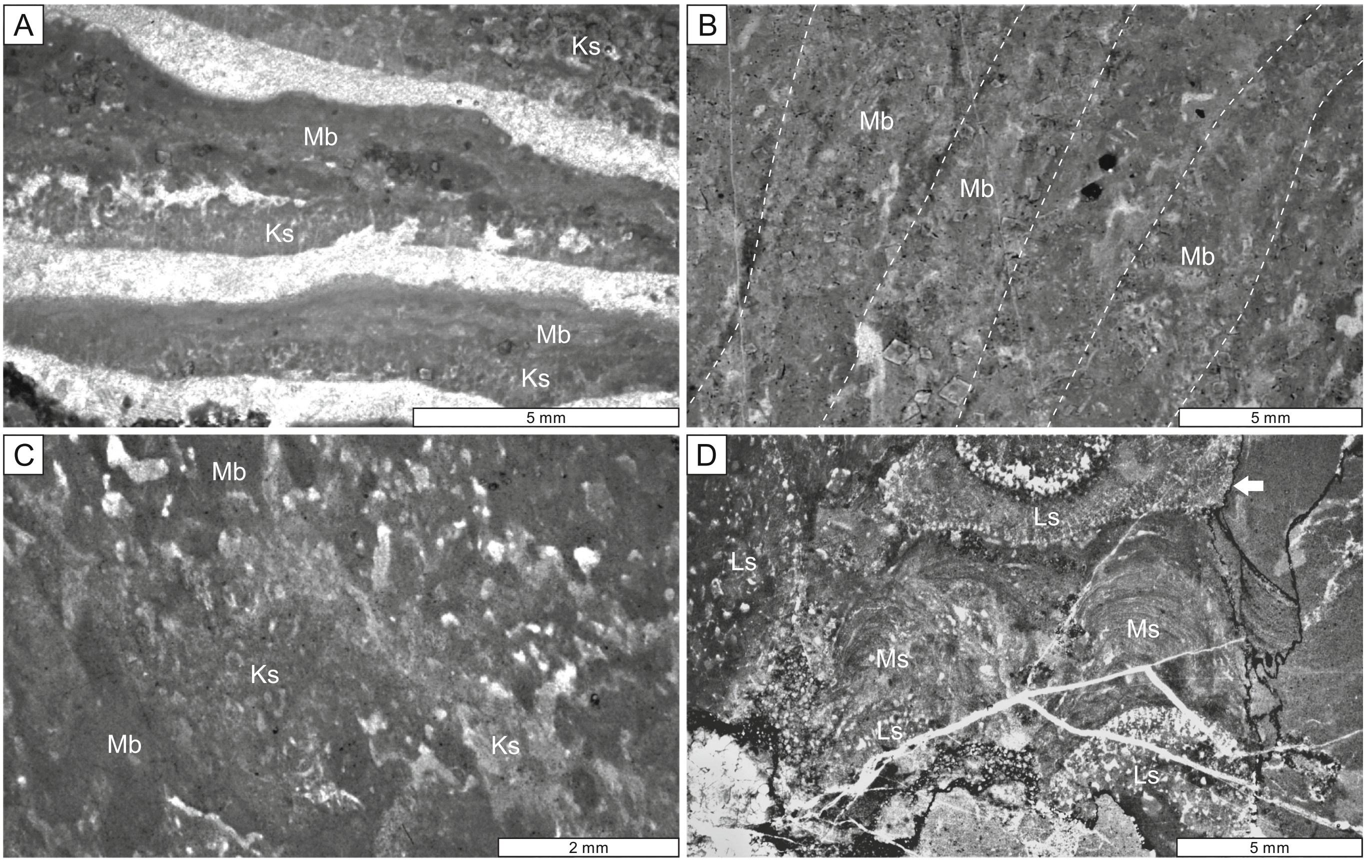

Fig. 5. Photomicrographs of microbial carbonate. (A) Thinly intercalated keratolite (Ks), laminated microbial carbonate (Mb), and blocky calcite layers forming the inner core of a stromatolite-like column. (B) Partially dolomitised microbial carbonate layers, forming the high-angled outer cover of a stromatolite-like column. Stromatolite layers are marked by white dotted lines. (C) Intermingled keratolites and minor microbial carbonates forming a keratolite–microbialite clot in a thrombolite-like mound. For location, see Fig. 4E. (D) Two columnar microstromatolites (Ms) encrusting underlying lithistid sponges (Ls) and overlain by the holdfast of the lithistid sponge *Archaeoscyphia* (white arrow) in a thrombolite-like mound.

to (Fig. 5A), and sometimes irregularly separates (Fig. 4A), the biogenic layers. The coarse sand-sized dolomite crystals commonly overlap primary biotic components and obscure their structures, but often follow and enhance layers of the stromatolite-like structure. The large crystal sizes of the calcite and dolomite suggest that these minerals were formed later in diagenesis (Amthor and Friedman, 1992; Montañez, 1994).

3.2. Macro- and mesostructures of the Mungok bioherms

3.2.1. Stromatolite-like columns

3.2.1.1. Description. The stromatolite-like structures are columnar in shape, with maximum widths and heights of 10 cm (Figs. 3B, 8). They overlie a thin oolitic grainstone bed and are overlain by bioclastic grainstone with a sharp erosive boundary (Fig. 3A, B). The stromatolite-like columns have ragged to straight lateral margins. The intercolumnar bioclastic packstone consists of lithistid sponges, bivalves, trilobites, crinoids, keratolite fragments, peloids, and intraclasts. The columns can be separated into two parts, an inner core consisting of low-angled layers (<45°) that are covered by high-angled layers (>45°) (Fig. 8B). The inner core can reach up to half to two-thirds of the column height, and is surrounded by the thinner (~2 cm thick) outer cover.

Keratolites and microbial carbonates are the two major biogenic components in the stromatolite-like columns. The inner core consists of laminoid keratolites that are often covered by microbial carbonate layers less than a millimetre thick forming small domes/columns, and then by sparry calcite layers 1–2 mm thick that frequently crosscut the keratolite/microbial carbonate layers (Figs. 4A–D, 5A). Keratolites, microbial carbonates, and sparry calcite layers repeatedly alternate (Figs. 4B, 5A) and form the columnar structure. The outer cover consists mainly of high-angled thin microbial carbonate layers with minor keratolites (Fig. 5B).

3.2.1.2. Interpretation. The coarse-grained intercolumnar sediments and truncation surface on the stromatolite together suggest that the stromatolite-like columns formed in a high-energy subtidal environment. In this environment, sponges may have grown as laminoid forms with a high basal area to volume ratio that helped them to adapt to the high-energy conditions (Kaandorp, 1999; Bell and Barnes, 2000; Meroz-Fine et al., 2005). Similar keratolite–microbial carbonate associations forming such stromatolite-like forms have been reported throughout Phanerozoic strata, but most commonly in upper Cambrian–Lower Ordovician rocks (Lee and Riding, 2021b, table 1). The thin micritic microbial carbonates encrusting the keratose sponges indicate the establishment of microbial communities associated with those sponges. Microbial mats can play an important role in the initial settlement of sponges by providing a suitable substrate (Whalan and Webster, 2014), and degraded sponge tissue supplies essential nutrients to microbial communities (Wilkinson and Fay, 1979; Sarà et al., 1998). The overall stromatolite-like fabrics were overprinted by selective recrystallization along the layered fabrics during the burial, resulting in the sparry calcite layers.

As the stromatolite-like columns expanded both vertically and laterally and formed the inner core, the intercolumnar spaces eventually became narrower and resulted in higher-energy hydrodynamic conditions. Such conditions would have been less favourable for sponges,

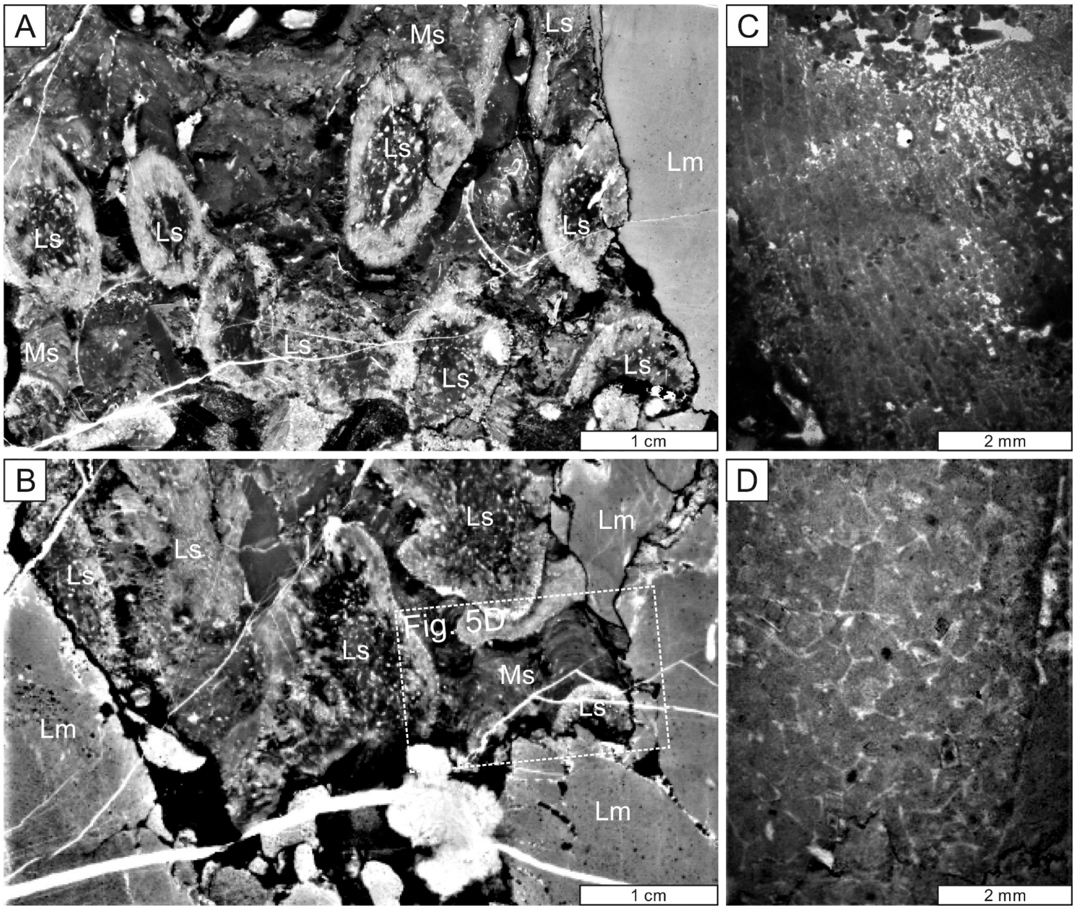

Fig. 6. Photomicrographs of the lithistid sponges in the thrombolite-like mounds. (A–B) Subvertically to horizontally oriented lithistid sponges (Ls), with some microstromatolites (Ms) encrusting lithistids. Homogeneous lime mud (Lm) surrounds the lithistid sponge–microstromatolite clots. (C) Longitudinal and (D) transverse sections of lithistid sponges. Note ladder-like spicule networks characteristic of anthaspidellid lithistids in (C).

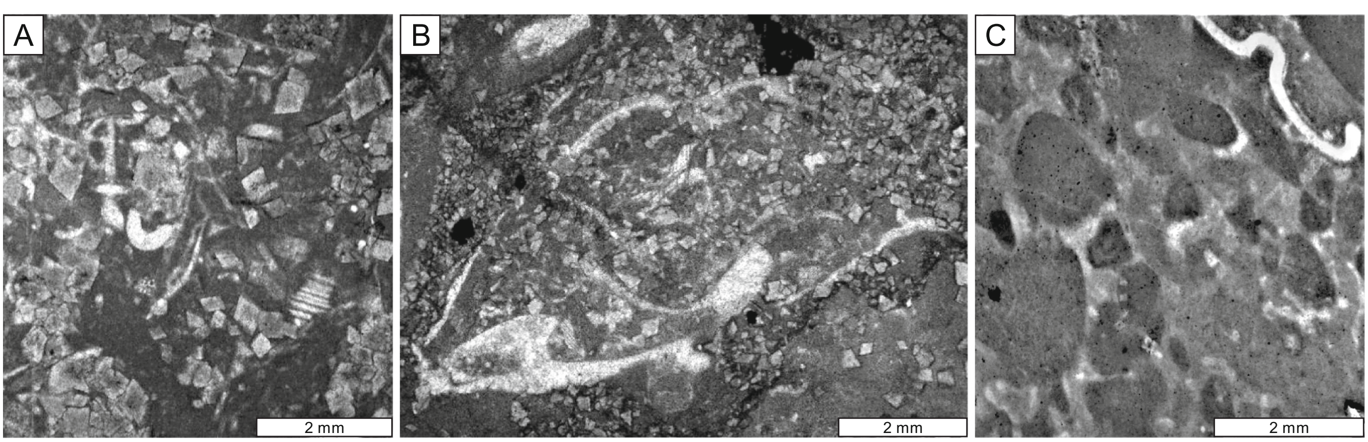

Fig. 7. Examples of the sediments between the Mungok bioherms. (A, B) Bioclastic packstone filling the space between the stromatolite-like columns, and containing (A) crinoids, trilobites, and (B) bivalves. (C) Micritic intraclasts and a trilobite fragment occurring between the thrombolite-like clots.

because of the requirement for higher pumping costs (Palumbi, 1984). In addition, strong currents or high waves often limit the morphological diversity of sponges in present-day environments (Bell and Barnes, 2000). In these circumstances, microbial carbonates would have covered the outer spaces of the inner core, forming the high-relief topography of the columns. Finally, the entire column became surrounded by coarse intercolumnar sediments and was subsequently eroded.

3.2.2. *Thrombolite-like mounds*

3.2.2.1. Description. The thrombolitic mounds are domes up to 100 cm high and 40–60 cm wide embedded within ribbon rock (Figs. 3C, 9). Mesoscale fabrics could not be observed in the field because of weathering and lichen growth. Analysis of slabs revealed that the mounds consist of cm-scale thrombolitic "clots" and homogeneous micrite with several intraclasts and bioclasts filling the interclot spaces (Fig. 9B). The

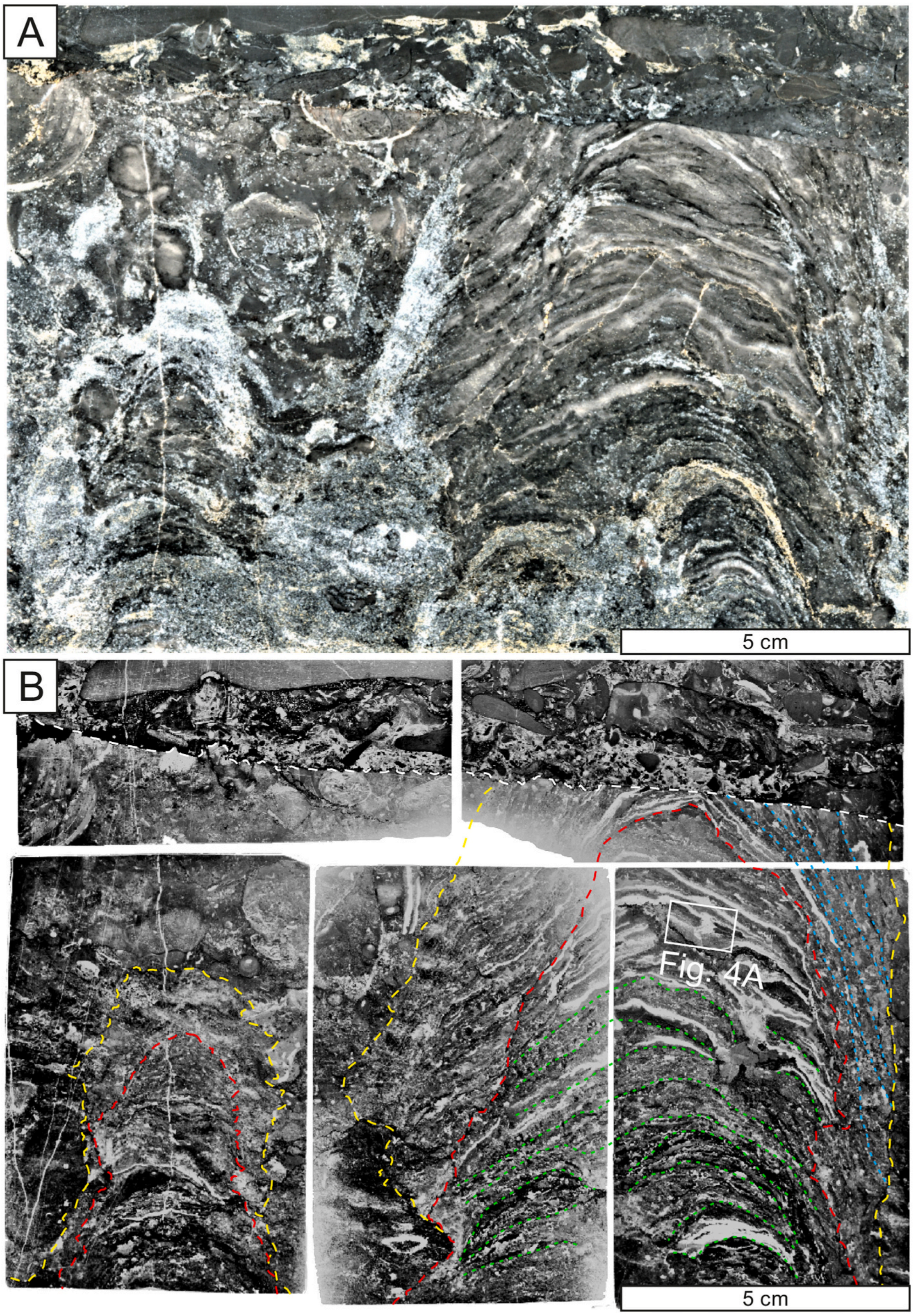

Fig. 8. Photographs of (A) a polished slab and (B) corresponding thin sections of stromatolite-like columns. Red and yellow dashed lines indicate the inner core and the outer cover of the stromatolite-like columns, respectively. Green and blue dotted lines show examples of low-angled layers (<45°) and high-angled layers (>45°), respectively. An erosive boundary (white dashed line) sharply truncates the stromatolite-like column on the right. (For interpretation of the references to colour in this figure legend, the reader is referred to the web version of this article.)

term clot is used here to indicate slab- to thin section-scale features of variable forms that superficially resemble mesoclots of thrombolites (Shapiro, 2000). The margins of clots are nearly vertical, clearly separating the clots from the interstitial micrites. Two types of clots are recognised: keratolite–microbialite and lithistid sponge–microstromatolite clots.

The keratolite–microbialite clots are irregular to bulbose in shape and ~5 cm wide and high, and are the most dominant component of the thrombolite-like mounds. They mainly consist of diffuse to dense networks of keratolite and small microbial carbonate patches embedded within the keratolites (Fig. 4E–G). The lithistid–microstromatolite clots are smaller than the keratolite–microbialite clots, and are usually a maximum of 1 cm wide and high. They occur in the spaces between the keratolite–microbialite clots and the ribbon rocks, and their boundaries are commonly overprinted by stylolites (Fig. 6). The lithistid sponges and microstromatolites encrust each other, forming rigid frameworks (Fig. 5D).

3.2.2.2. Interpretation. The thrombolite-like mounds formed in a low-energy subtidal environment, probably below normal wave base, where ribbon rocks of lime mudstone and shale were deposited (Chen et al., 2010; Bayet-Goll et al., 2015). The low-energy conditions would have promoted growth of keratose sponges in a variety of morphologies such as irregular to bulbose clots (Bell and Barnes, 2000). We infer that the bulbose growth forms of keratose sponges would have resulted in the overall shapes of the keratolite–microbialite clots. Microclotted micrites may have been formed from the degrading sponge soft tissue (Reitner, 1993; Guido et al., 2019). Microstromatolites and lithistid sponges would have grown in the limited spaces between the keratolite–microbialite clots. The sponges and microstromatolites grew on each other, forming the lithistid–microstromatolite clots (Hong et al., 2016; Lee et al., 2019).

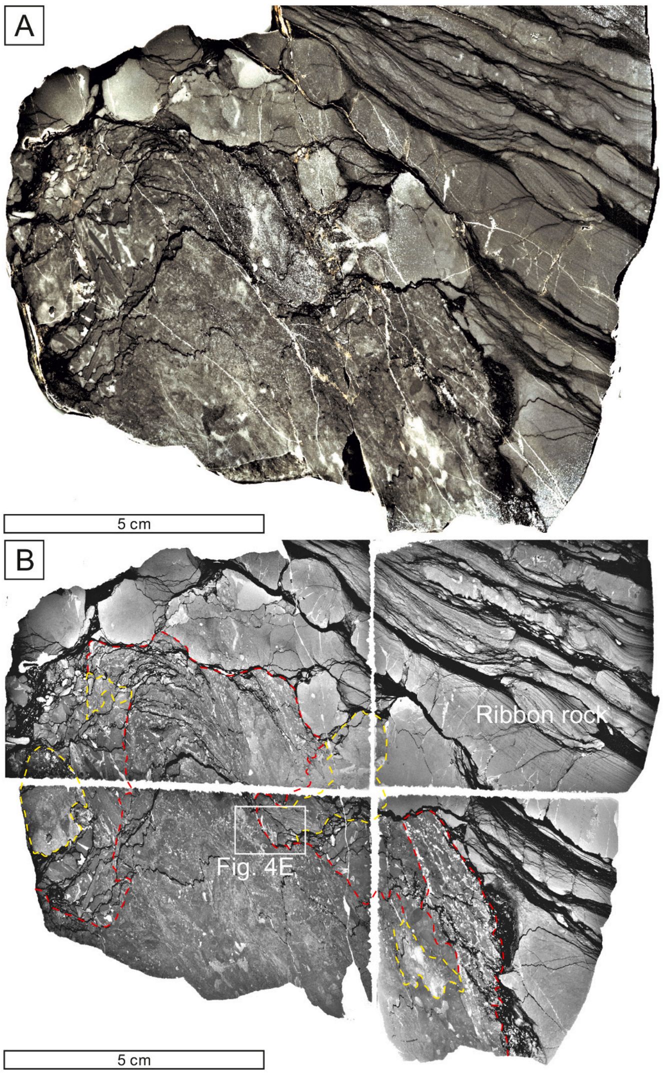

Fig. 9. Photographs of (A) a polished slab and (B) corresponding thin sections of the thrombolite-like mounds. Irregular to bulbous keratose–microbial clots (red dashed lines) and lithistid–microstromatolite clots (yellow dashed lines) are surrounded by ribbon rocks composed of alternating lime mudstone and shale beds. (For interpretation of the references to colour in this figure legend, the reader is referred to the web version of this article.)

4. Discussion

The sponge–microbial carbonate reef-building consortium is characteristic of the Furongian (late Cambrian) to Early Ordovician. During that time, high temperatures and low dissolved oxygen concentrations limited diversification of other metazoan reef builders (Lee and Riding, 2018). Lithistid–microbial reefs are thought to have been the most important reef type of this time interval (Lee et al., 2016a; Lee and Riding, 2018), together with recently recognised keratosan–microbial reefs. During the Early Ordovician, newly appearing metazoan reef-builders, including calathiids, bryozoans, coralomorphs (e.g., *Amsassia*), and pulchrilaminids, augmented these sponge–microbial reefs, but were still minor reef components (e.g., Toomey and Ham, 1967; Cañas and Carrera, 1993; Keller and Flügel, 1996; Adachi et al., 2012; Cuffey et al., 2013; Li et al., 2014, 2015; Carrera et al., 2017; Shen and Neuweiler, 2018; Elias et al., 2021).

Keratolite–microbialite associations occurred throughout the Phanerozoic, but were especially common during the Cambrian–Ordovician, Middle Devonian–Mississippian (early Carboniferous), and Early Triassic, when microbial carbonates were abundant (Lee and Riding, 2021b, fig. 9). In the Furongian, keratosans became important reef-builders in microbialite-dominant reefs, forming maze-like maceriate reefs (Lee et al., 2014) and/or stromatolite-like structures (Lee and Riding, 2021b and references therein), but remained cryptic dwellers in lithistid–microbial reefs (Lee et al., 2019). Keratose sponges became less important during the Early Ordovician, though they were still essential cryptic dwellers within lithistid–microbial reefs (Hong et al., 2014; Li et al., 2017) or formed stromatolite-like structures by the intergrowth of keratosans and microbial carbonates (Li et al., 2019a). Overall, these examples suggest that keratosans could have played an essential role in reef-building during this time of sponge–microbial reef dominance (Lee and Riding, 2018).

The Mungok bioherms demonstrate how the shapes of keratose sponge–microbial reef-building associations could change in different depositional environments (Fig. 10). In higher-energy hydrodynamic conditions, keratose sponges and microbes formed a stromatolite-like tight laminar frame reef (sensu Riding, 2002) (Table 1). In contrast, thrombolite-like mounds consisting of bulbose keratosans with minor lithistid–microbial clots developed in low-energy conditions (Table 1); these assemblages are interpreted as cluster reefs (sensu Riding, 2002). The other Early Ordovician lithistid–microbial–calathiid reefs with grainstone talus that have been described from various palaeocontinents (e.g., Cañas and Carrera, 1993; Adachi et al., 2009; Choh et al., 2013; Li et al., 2015) (Table 1) can be classified as domical open frame reefs (sensu Riding, 2002) and developed in high-energy environments, though the common presence of allomicrites between the reefal frameworks suggests relatively lower-energy conditions than for the stromatolite-like columns. These examples collectively demonstrate the relationship between reef composition/structure and hydrodynamic

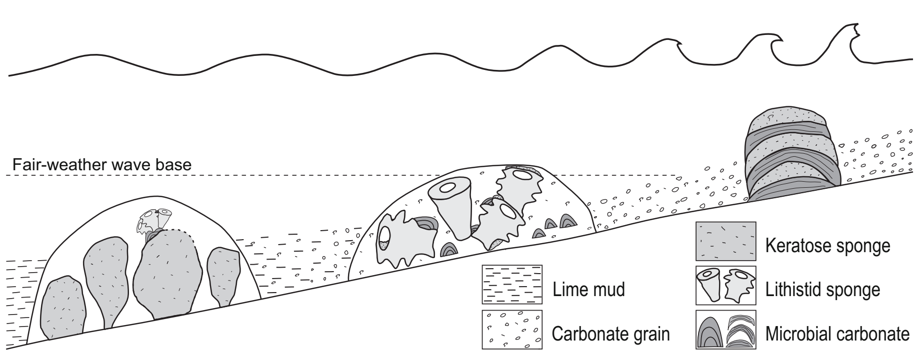

Fig. 10. Schematic diagram of sponge–microbial reef distribution in different hydrodynamic conditions during the Furongian to the Early Ordovician based on the information in Table 1. Keratosan thrombolite-like mounds, lithistid–microbial reefs, and keratosan–microbial stromatolite-like columns occur in low-, intermediate-, and high-energy conditions, respectively. Not to scale.

Table 1
Summary of Furongian (late Cambrian)–Early Ordovician sponge–microbial reefs. Hydrodynamic conditions are estimated based on the depositional environments and composition of inter-reef sediments. Fm., Formation; fms., formations.

Age	Location	Reef description	Depositional environment	Inter-reef sediment	Hydrodynamic conditions	Reference
Early Ordovician (Floian)	McKelligon Canyon Fm., Southern Franklin Mountain, West Texas, USA	Carbonate mound with lithistid sponge (*Archaeoscyphia*), *Calathium*, *Pulchrilamina*, and minor microbialites	Shallow intertidal to subtidal	Skeletal wackestone; intraclastic and bioclastic wackestone–packstone–grainstone	Intermediate	Toomey (1970)
Early Ordovician (Floian)	Romaine Fm., Mingan Island, Québec, Canada	Thrombolitic mound with anthaspidellid demosponges	Shallow marine	Grainstone	High–intermediate	Rigby and Desrochers (1995)
Early Ordovician (late Floian)	Fillmore Fm., western central Utah, USA	"Wyatt's reef"; micrite and some sponges	Shallow lagoon or bay	Bioturbated lime mudstone and wackestone	Low	Wyatt (1979), Miller et al. (2012)
Early Ordovician (middle Floian)	Fillmore Fm., western central Utah, USA	"*Calathium* reef"; mainly *Calathium* with few anthaspidellid sponges	Shelf	No data	Unknown	Miller et al. (2012)
Early Ordovician (early Floian)	Lower Setul Limestone, Perlis, Malaysia	Keratose sponge-bearing microbialite with minor lithistid sponges and *Calathium*	Shallow subtidal	Thick-bedded skeletal pack/ grainstone	High	Li et al. (2019b)
Early Ordovician (early Floian)	Dumugol Fm., Taebaek, South Korea	Lithistid sponge (*Archaeoscyphia*)–*Calathium*–microbial reef with minor cryptic keratose sponges	Inner to mid ramp	Thin-bedded lime mudstone with intraclastic/bioclastic pack/ grainstone	Intermediate	Kwon et al. (2003), Choh et al. (2013), Hong et al. (2014, 2015)
Early Ordovician (late Tremadocian–early Floian	Hunghuayuan Fm., Anhui, China	Microbial–lithistid sponge–receptaculitid reef	Shallow to deep marine	Bioclastic limestone	Unknown (intermediate?)	Adachi et al. (2009)
Early Ordovician (late Tremadocian–early Floian)	Hunghuayuan Fm., Guizhou, China	Lithistid sponge–*Calathium* reef with cryptic keratose sponges, stromatoporoids (*Cystostroma*), *Pulchrilamina*, and bryozoans	Shallow marine (outer shelf)	Bioclastic packstone	Intermediate	Li et al. (2014, 2017)
Early Ordovician (late Tremadocian–early Floian)	San Juan Fm., Argentina	Microbial–lithistid sponge–receptaculitid reefs	Subtidal	Skeletal/peloidal/intraclastic pack/ wackestone with minor grainstone lens	Intermediate	Cañas and Carrera (1993)
Early Ordovician (late Tremadocian)	Survey Peak Fm., Rocky Mountains, Alberta, Canada	Thrombolite mound with lithistid sponges	Open carbonate shelf	Thin-bedded grainstone and lime mudstone with various bioclastic fragments and intraclasts	Intermediate	Pratt (1989)
Early Ordovician (late Tremadocian)	Fenhsiang Fm., Chenjiahe, Hubei, South China	Lithistid sponge–microbial reef with local *Calathium*, bryozoans, *Pulchrilamina*, and bioclastic wackestone	Shallow marine to deeper-water	Bioclastic limestone with abundant pelmatozoans and trilobites	Intermediate	Adachi et al. (2011)
Early Ordovician (late Tremadocian)	Pa Nan Fm., Tarutao Islands, Satun Province, Thailand	Massive "stromatolite"; keratose sponges and tubiform calcimicrobes	Shallow subtidal	Bioclastic limestone	Unknown	Li et al. (2019a)
Early Ordovician (late Tremadocian)	Fillmore Fm., western central Utah, USA	"Church's reef"; anthaspidelid sponges with few *Calathium*	Shallow shelf	Bioclastic limestone and intraformational conglomerate	High–intermediate	Church (1974), Kröger and Penny, 2020
Early Ordovician (middle Tremadocian)	Fillmore Fm., western central Utah, USA	"Hintze's reef"; mainly thrombolites with anthaspidellid sponges	Shallow shelf	No data	Unknown	Miller et al. (2012)
Early Ordovician (middle Tremadocian)	Fillmore Fm., western central Utah, USA	"Miller's reef"; stromatolites with minor anthaspidellid sponges	Shallow shelf	Bioclastic grainstone	High (?)	Miller et al. (2012)
Early Ordovician (early Tremadocian)	Mungok Fm., Yeongwol, Korea	Stromatolite-like columns of keratolites and microbial carbonates	Shallow subtidal	Bioclastic grainstone	High	This study
Early Ordovician (early Tremadocian)	Mungok Fm., Yeongwol, Korea	Thrombolite-like mound of keratolite–microbial carbonate with limited lithistid sponges–microstromatolites	Deep subtidal	Limestone–shale couplets	Low	This study
Late Cambrian (Stage 10)–Early Ordovician (Tremadocian)	Berry Head and Watts Bight fms., Newfoundland, Canada	Columnar and domical keratolite–stromatolite consortia	Shallow marine	Intraclastic grainstone and micrite	High–intermediate	Lee and Riding (in press)
Late Cambrian (Stage 10)	Little Falls Fm., New York, USA	*Cryptozoön* "stromatolite"; alternating keratolites and microbial carbonates	Shallow shelf	Oolitic grainstone	High	Lee and Riding (2021a)
Late Cambrian (Stage 10)	Chaomidian Fm., Shandong, China	Stromatolite with keratose sponges, microstromatolites and *Girvanella*	High-energy shallow subtidal	Bioclastic grainstone	High	Chen et al. (2014)

(*continued on next page*)

Table 1 (*continued*)

Age	Location	Reef description	Depositional environment	Inter-reef sediment	Hydrodynamic conditions	Reference
Late Cambrian (Stage 10)	Notch Peak Fm., Nevada, USA	Lithistid sponge–microstromatolite reef with minor cryptic keratose sponges	Carbonate platform	Partly dolomitised and bioturbated lime mudstone–wackestone	Low–intermediate	Lee et al. (2019)
Late Cambrian (Jiangshanian)	Wilberns Fm., Colorado, USA	Lithistid sponge (*Wilbernicyathus*)–microbial reef	Shallow marine	No data	Intermediate–high (?)	Johns et al. (2007)
Late Cambrian (Jiangshanian)	Notch Peak Fm., Nevada, USA	Keratose sponge–microbial reef (originally described as a lithistid sponge–microbial reef)	Carbonate platform	Intra-bioclastic grainstone with minor packstone	High	Coulson and Brand (2016)
Late Cambrian (Jiangshanian)	Chaomidian Fm., Shandong, China	Maceriate reef formed by keratose sponges and microbes	Shallow marine	Lime mud with few bioclasts	Low	Lee et al. (2014)
Late Cambrian (Jiangshanian)	Chaomidian Fm., Beijing, China	Maceriate reef formed by keratose sponges and microbes	Shallow subtidal	Micrite with minor bioclasts	Low	Chen et al. (2014)
Late Cambrian (Paibian)	Bonanza King Fm., Nevada/ California, USA	Lithistid sponge (*Gallatinospongia*)–dendrolite	Shallow subtidal ramp	No data	High	Shapiro and Rigby (2004)
Late Cambrian (Paibian)	Deh-Molla Fm., Iran	Lithistid sponge (*Rankenella*)–*Girvanella*	Subtidal	Bioclastic packstone with lime mud	Intermediate	Kruse and Zhuravlev (2008)

conditions during the Furongian to the Early Ordovician (Fig. 10).

Interestingly, the aforementioned examples suggest that there may be an inverse correlation between the abundances of reef-building keratosans and lithistids. Keratosans are generally less important in lithistid–microbial reefs and were mainly present as cryptic dwellers (Hong et al., 2015; Lee et al., 2016a, 2019; Li et al., 2017), except for a single example of a Lower Ordovician lithistid–microbial reef in South Korea, in which keratosans performed diverse roles, including as cryptic dwellers, encrusters, and as partial framebuilders (Hong et al., 2015) (Table 1). In contrast, lithistids are either absent or seldomly found in keratolite–microbial carbonate reefs (e.g., Lee et al., 2014; Li et al., 2019a) (Table 1). Such examples suggest that there could have been niche partitioning between the lithistid–microbial and keratosan–microbial associations; the limited number of cases necessitates additional studies to support this interpretation. This niche partitioning could have been caused by competition for resources such as food or space, or differential adaptation to environments with various hydrodynamic conditions. The morphological similarities of keratosan–microbial reefs to stromatolites and thrombolites suggest that there should be many unknown examples of keratosan–microbial consortia in the geological record, especially in lower Palaeozoic successions. Further detailed studies of such "microbialites" may help us to reveal the yet unknown palaeoecological roles of keratosan–microbial consortia in reef ecosystems during the GOBE.

5. Conclusions

The Lower Ordovician stromatolite-like columns and thrombolite-like mounds of the Mungok Formation were constructed mainly by keratose sponges and microbes. The stromatolite-like columns consist of keratolites and microbial carbonates, which encrusted one another and formed the stromatolitic laminae. The thrombolite-like clots were built by irregular to bulbous keratosan–microbial associations with limited lithistid–microbial elements. The superficial similarities between the keratosan–microbial consortium and microbialites could have hindered the identification of keratosan–microbial reefs in the geological record.

Sponge–microbial consortia, with lithistids and with keratosans, were dominant reef-builders throughout the Furongian–Early Ordovician. The results of the present study, together with other recent reports of keratosan–microbial associations, suggest that such associations could have been a critical element of reef ecosystems during the early Palaeozoic. The keratosan–microbial consortium could have inhabited environments different from those of the lithistid–microbial consortium, indicating possible niche separation. The Mungok bioherms provide new examples of keratose sponge–microbial reefs, and help us to reconstruct the evolutionary history of reefs during the GOBE.

Declaration of Competing Interest

The authors declare that they have no known competing financial interests or personal relationships that could have appeared to influence the work reported in this paper.

Acknowledgements

This manuscript is based on the first author's MSc thesis. We thank G. S. Chung for introducing us to the outcrop and S.K. Yang for sample preparation. Comments from J. Reitner, two anonymous reviewers and the editor I. Montañez are very much appreciated. This study was supported by National Research Foundation of Korea grants to JHL (2018R1A4A1059956 and 2019R1A2C4069278) and to JH (2019R1A6A1A03033167 and 2020R1C1C1007690). This paper is a contribution to IGCP Project 735 "Rocks and the Rise of Ordovician Life: Filling knowledge gaps in the Early Palaeozoic Biodiversification".

References

Adachi, N., Ezaki, Y., Liu, J., Cao, J., 2009. Early Ordovician reef construction in Anhui Province, South China: A geobiological transition from microbial- to metazoan-dominant reefs. Sediment. Geol. 220, 1–11. https://doi.org/10.1016/j.sedgeo.2009.05.012.

Adachi, N., Ezaki, Y., Liu, J., 2011. Early Ordovician shift in reef construction from microbial to metazoan reefs. Palaios 26, 106–114. https://doi.org/10.2110/palo.2010.p10-097r.

Adachi, N., Liu, J., Ezaki, Y., 2012. Early Ordovician stromatoporoid *Pulchrilamina spinosa* from South China: Geobiological significance and implications for the early development of skeletal-dominated reefs. Paleontol. Res. 16, 59–69. https://doi.org/10.2517/1342-8144-16.1.059.

Amthor, J.E., Friedman, G.M., 1992. Early- to late-diagenetic dolomitization of platform carbonates; Lower Ordovician Ellenburger Group, Permian Basin, West Texas. J. Sediment. Petrol. 62, 131–144. https://doi.org/10.1306/D42678AC-2B26-11D7-8648000102C1865D.

Arp, G., Reimer, A., Reitner, J., 2001. Photosynthesis-induced biofilm calcification and calcium concentrations in Phanerozoic oceans. Science 292, 1701–1704. https://doi.org/10.1126/science.1057204.

Bayet-Goll, A., Chen, J., Moussavi-Harami, R., Mahboubi, A., 2015. Depositional processes of ribbon carbonates in Middle Cambrian of Iran (Deh-Sufiyan Formation, Central Alborz). Facies 61, 9. https://doi.org/10.1007/s10347-015-0436-6.

Bell, J.J., Barnes, D.K.A., 2000. The influences of bathymetry and flow regime upon the morphology of sublittoral sponge communities. J. Mar. Biol. Assoc. U. K. 80, 707–718. https://doi.org/10.1017/s0025315400002538.

Bertrand-Sarfati, J., 1976. An attempt to classify Late Precambrian stromatolite microstructures. In: Walter, M.R. (Ed.), Stromatolites. Developments in Sedimentology, 20. Elsevier, pp. 251–259. https://doi.org/10.1016/s0070-4571(08)71138-5.

Brunton, F.R., Dixon, O.A., 1994. Siliceous sponge-microbe biotic associations and their recurrence through the Phanerozoic as reef mound constructors. Palaios 9, 370–387. https://doi.org/10.2307/3515056.

Cañas, F., Carrera, M., 1993. Early Ordovician microbial-sponge-receptaculitid bioherms of the Precordillera, Western Argentina. Facies 29, 169–178. https://doi.org/10.1007/BF02536927.

Carrera, M.G., Astini, R.A., Gomez, F.J., 2017. A lowermost Ordovician tabulate-like coralomorph from the Precordillera of western Argentina: a main component of a reef-framework consortium. J. Paleontol. 91, 73–85. https://doi.org/10.1017/jpa.2016.145.

Chen, J., Han, Z., Zhang, X., Fan, A., Yang, R., 2010. Early diagenetic deformation structures of the Furongian ribbon rocks in Shandong Province of China—A new perspective of the genesis of limestone conglomerates. Sci. China Earth Sci. 53, 241–252. https://doi.org/10.1007/s11430-010-0010-6.

Chen, J., Lee, J.-H., Woo, J., 2014. Formative mechanisms, depositional processes, and geological implications of Furongian (late Cambrian) reefs in the North China Platform. Palaeogeogr. Palaeoclimatol. Palaeoecol. 414, 246–259. https://doi.org/10.1016/j.palaeo.2014.09.004.

Cho, H.S., Kim, J.Y., 2007. Graptolite biostratigraphy and its correlation of the Mungok and Yeonghung formations at Yeongwol area, Korea. Geosci. J. 11, 23–38. https://doi.org/10.1007/BF02910378.

Choh, S.-J., Hong, J., Sun, N., Kwon, S.-W., Park, T.-Y., Woo, J., Kwon, Y.K., Lee, D.-C., Lee, D.-J., 2013. Early Ordovician reefs from the Taebaek Group, Korea: constituents, types, and geological implications. Geosci. J. 17, 139–149. https://doi.org/10.1007/s12303-013-0024-0.

Choi, D.K., 1998. The Yongwol Group (Cambrian-Ordovician) redefined: a proposal for the stratigraphic nomenclature of the Choson Supergroup. Geosci. J. 2, 220–234. https://doi.org/10.1007/BF02910166.

Choi, D.K., 2019. Evolution of the Taebaeksan Basin, Korea: I, early Paleozoic sedimentation in an epeiric sea and break-up of the Sino-Korean Craton from Gondwana. Island Arc 28. https://doi.org/10.1111/iar.12275.

Choi, D.K., Chough, S.K., 2005. The Cambrian-Ordovician stratigraphy of the Taebaeksan Basin, Korea: a review. Geosci. J. 9, 187–214. https://doi.org/10.1007/BF02910579.

Choi, D.K., Kim, D.H., Sohn, J.W., 2001. Ordovician trilobite faunas and depositional history of the Taebaeksan Basin, Korea: implications for palaeogeography. Alcheringa 25, 53–68. https://doi.org/10.1080/03115510108619213.

Chough, S.K., 2013. Geology and Sedimentology of Korean Peninsula. Elsevier Insights, Elsevier. https://doi.org/10.1016/C2012-0-02847-5, 363 pp.

Chough, S.K., Kwon, S.T., Ree, J.-H., Choi, D.K., 2000. Tectonic and sedimentary evolution of the Korean peninsula: a review and new view. Earth Sci. Rev. 52, 175–235. https://doi.org/10.1016/s0012-8252(00)00029-5.

Church, S.B., 1974. Lower Ordovician patch reefs in western Utah. Brigham Young Univ. Geol. Stud. 21, 41–62. https://doi.org/10.1017/S0022336000030699.

Church, S.B., 2017. Efficient ornamentation in Ordovician anthaspidellid sponges. Paleontol. Contrib. 18, 1–8. https://doi.org/10.17161/1808.24771.

Cluzel, D., Jolivet, L., Cadet, J.-P., 1991. Early Middle Paleozoic intraplate orogeny in the Ogcheon Belt (South Korea): a new insight on the Paleozoic buildup of east Asia. Tectonics 10, 1130–1151. https://doi.org/10.1029/91TC00866.

Copper, P., 2011. 100 million years of reef prosperity and collapse: Ordovician to Devonian interval. In: Stanley, G.D. (Ed.), Corals and Reef Crises, Collapse and Change, The Paleontological Society Special Papers, 17, pp. 15–32. https://doi.org/10.1017/s1089332600002424.

Cordie, D.R., Dornbos, S.Q., Marenco, P.J., 2019. Increase in carbonate contribution from framework-building metazoans through Early Cambrian reefs of the Western Basin and Range, USA. Palaios 34, 159–174. https://doi.org/10.2110/palo.2018.085.

Coulson, K.P., Brand, L.R., 2016. Lithistid sponge-microbial reef-building communities construct laminated, Upper Cambrian (Furongian) 'stromatolites'. Palaios 31, 358–370. https://doi.org/10.2110/palo.2016.029.

Cuffey, R.J., Chuantao, X., Zhu, Z., Spjeldnaes, N., Hu, Z.-X., 2013. The world's oldest-known bryozoan reefs: late tremadocian, mid-early Ordovician; Yichang, central China. In: Ernst, A., Schäfer, P., Scholz, J. (Eds.), Bryozoan Studies 2010. Springer-Verlag, Berlin/Heidelberg, pp. 13–27.

Elias, R.J., Lee, D.-J., Pratt, B.R., 2021. The "earliest tabulate corals" are not tabulates. Geology 49, 304–308. https://doi.org/10.1130/g48235.1.

Gandin, A., Debrenne, F., 2010. Distribution of the archaeocyath-calcimicrobial bioconstructions on the Early Cambrian shelves. Palaeoworld 19, 222–241. https://doi.org/10.1016/j.palwor.2010.09.010.

Goldman, D., Sadler, P.M., Leslie, S.A., Melchin, M.J., Agterberg, F.P., Gradstein, F.M., 2020. The Ordovician Period. In: Gradstein, F.M., Ogg, J.G., Schmitz, M.D., Ogg, G. M. (Eds.), Geologic Time Scale 2020. Elsevier, pp. 631–694.

Guido, A., Gerovasileiou, V., Russo, F., Rosso, A., Sanfilippo, R., Voultsiadou, E., Mastandrea, A., 2019. Composition and biostratinomy of sponge-rich biogenic crusts in submarine caves (Aegean Sea, Eastern Mediterranean). Palaeogeogr. Palaeoclimatol. Palaeoecol. 534, 109338. https://doi.org/10.1016/j.palaeo.2019.109338.

Harwood, C.L., Sumner, D.Y., 2012. Origins of microbial microstructures in the Neoproterozoic Beck Spring Dolomite: variations in microbial community and timing of lithification. J. Sediment. Res. 82, 709–722. https://doi.org/10.2110/jsr.2012.65.

Hong, J., Choh, S.-J., Lee, D.-J., 2014. Tales from the crypt: early adaptation of cryptobiontic sessile metazoans. Palaios 29, 95–100. https://doi.org/10.2110/palo.2014.076.

Hong, J., Choh, S.-J., Lee, D.-J., 2015. Untangling intricate microbial–sponge frameworks: the contributions of sponges to Early Ordovician reefs. Sediment. Geol. 318, 75–84. https://doi.org/10.1016/j.sedgeo.2015.01.003.

Hong, J., Lee, J.-H., Choh, S.-J., Lee, D.-J., 2016. Cambrian Series 3 carbonate platform of Korea dominated by microbial-sponge reefs. Sediment. Geol. 341, 58–69. https://doi.org/10.1016/j.sedgeo.2016.04.012.

Johns, R.A., Dattilo, B.F., Spincer, B., 2007. Neotype and redescription of the Upper Cambrian anthaspidellid sponge, *Wilbernicyathus donegani* Wilson, 1950. J. Paleontol. 81, 435–444. https://doi.org/10.1666/05028.1.

Kaandorp, J.A., 1999. Morphological analysis of growth forms of branching marine sessile organisms along environmental gradients. Mar. Biol. 134, 295–306. https://doi.org/10.1007/s002270050547.

Keller, M., Flügel, E., 1996. Early Ordovician reefs from Argentina: stromatoporoid vs stromatolite origin. Facies 34, 177–192. https://doi.org/10.1007/BF02546163.

Kershaw, S., 2015. Paleoecology of the Paleozoic Stromatoporoidea. In: Stearn, C.W. (Ed.), Treatise on Invertebrate Paleontology, Part E, Porifera, Revised, Hypercalcified Porifera, Volumes 4 and 5. The University of Kansas Paleontological Institute, Lawrence, Kansas, pp. 631–651. https://doi.org/10.17161/to.v0i0.4253.

Kershaw, S., Munnecke, A., Jarochowska, E., 2018. Understanding Palaeozoic stromatoporoid growth. Earth Sci. Rev. 187, 53–76. https://doi.org/10.1016/j.earscirev.2018.08.003.

Keupp, H., Jenisch, A., Herrmann, R., Neuweiler, F., Reitner, J., 1993. Microbial carbonate crusts - a key to the environmental analysis of fossil spongiolites? Facies 29, 41–54. https://doi.org/10.1007/BF02536916.

Kim, D.H., Choi, D.K., 2000. Lithostratigraphy and biostratigraphy of the Mungok Formation (Lower Ordovician), Yongwol, Korea. Geosci. J. 4, 301–311.

Kim, Y.-H.G., Rhee, C.W., Woo, J., Park, T.-Y.S., 2014. Depositional systems of the Lower Ordovician Mungok Formation in Yeongwol, Korea: implications for the carbonate ramp facies development. Geosci. J. 18, 397–417. https://doi.org/10.1007/s12303-014-0033-7.

Knoll, A.H., Semikhatov, M.A., 1998. The genesis and time distribution of two distinctive Proterozoic stromatolite microstructures. Palaios 13, 408–422. https://doi.org/10.2307/3515471.

Kobayashi, T., 1966. The Cambro-Ordovician formations and faunas of South Korea, Part X, Stratigraphy of the Chosen Group in Korea and South Manchuria and its relation to the Cambro-Ordovician formations of other areas, Section A. The Chosen Group of South Korea. J. Fac. Sci. University of Tokyo, Section II 16, 1–84.

Kröger, B., Desrochers, A., Ernst, A., 2017. The reengineering of reef habitats during the Great Ordovician Biodiversification Event. Palaios 32, 584–599. https://doi.org/10.2110/palo.2017.017.

Kröger, B., Penny, A., 2020. Early–Middle Ordovician Seascape-Scale aggregation pattern of sponge-rich reefs across the Laurentia paleocontinent. Palaios 35, 524–542. https://doi.org/10.2110/palo.2020.039.

Kruse, P.D., Zhuravlev, A.Y., 2008. Middle–Late Cambrian *Rankenella-Girvanella* reefs of the Mila formation, northern Iran. Can. J. Earth Sci. 45, 619–639. https://doi.org/10.1139/e08-016.

Kwon, Y.K., 2012. Sequence stratigraphy of the Yeongweol Group (Cambrian-Ordovician), Taebaeksan Basin, Korea: paleogeographic implications. Econ. Environ. Geol. 45, 317–333. https://doi.org/10.9719/EEG.2012.45.3.317.

Kwon, Y.K., Lee, D.J., Choi, D.K., Chough, S.K., 2003. Lower Ordovician sponge bioherms in the Makkol Formation, Taebaeksan Basin, Mideast Korea. Facies 48, 79–90. https://doi.org/10.1007/BF02667531.

Lee, J.-G., 1995. Late Cambrian trilobites from the Machari Formation, Yeongweol, Korea. Ph.D. Thesis. Seoul National University, Seoul (418 pp).

Lee, J.-H., 2020a. A preliminary study on so-called "Mungokri stromatolite", Natural Monument No. 413 of South Korea: possibility of abiotic origin. J. Geol. Soc. Korea 56, 365–373. https://doi.org/10.14770/jgsk.2020.56.3.365 (in Korean with English abstract).

Lee, S.-B., 2020b. *Kayseraspis* (Trilobita) from the Mungok Formation in Yeongwol area and its significance for the Lower Ordovician biostratigraphy and chronostratigraphy of the Taebaeksan Basin, Korea. Geosci. J. 24, 351–357. https://doi.org/10.1007/s12303-020-0009-8.

Lee, J.-H., Riding, R., 2018. Marine oxygenation, lithistid sponges, and the early history of Paleozoic skeletal reefs. Earth Sci. Rev. 181, 98–121. https://doi.org/10.1016/j.earscirev.2018.04.003.

Lee, J.-H., Riding, R., 2021a. The 'classic stromatolite' *Cryptozoön* is a keratose sponge-microbial consortium. Geobiology 19, 189–198. https://doi.org/10.1111/gbi.12422.

Lee, J.-H., Riding, R., 2021b. Keratolite–stromatolite consortia mimic domical and branched columnar stromatolites. Palaeogeogr. Palaeoclimatol. Palaeoecol. 571, 110288. https://doi.org/10.1016/j.palaeo.2021.110288.

Lee, J.-H., Chen, J., Choh, S.-J., Lee, D.-J., Han, Z., Chough, S.K., 2014. Furongian (late Cambrian) sponge-microbial maze-like reefs in the North China Platform. Palaios 29, 27–37. https://doi.org/10.2110/palo.2013.050.

Lee, J.-H., Chen, J., Chough, S.K., 2015. The middle–late Cambrian reef transition and related geological events: a review and new view. Earth Sci. Rev. 145, 66–84. https://doi.org/10.1016/j.earscirev.2015.03.002.

Lee, J.-H., Hong, J., Choh, S.-J., Lee, D.-J., Woo, J., Riding, R., 2016a. Early recovery of sponge framework reefs after Cambrian archaeocyath extinction: Zhangxia Formation (early Cambrian Series 3), Shandong, North China. Palaeogeogr. Palaeoclimatol. Palaeoecol. 457, 269–276. https://doi.org/10.1016/j.palaeo.2016.06.018.

Lee, J.-H., Hong, J., Lee, D.-J., Choh, S.-J., 2016b. A new Middle Ordovician bivalve–siliceous sponge–microbe reef-building consortium from North China. Palaeogeogr. Palaeoclimatol. Palaeoecol. 457, 23–30. https://doi.org/10.1016/j.palaeo.2016.05.034.

Lee, J.-H., Dattilo, B.F., Mrozek, S., Miller, J.F., Riding, R., 2019. Lithistid sponge-microbial reefs, Nevada, USA: filling the late Cambrian 'reef gap'. Palaeogeogr.

Palaeoclimatol. Palaeoecol. 520, 251–262. https://doi.org/10.1016/j.palaeo.2019.02.003.

Li, Q., Li, Y., Kiessling, W., 2014. Early Ordovician sponge-*Calathium*-microbial reefs on the Yangtze Platform margin of the South China Block. Gff 136, 157–161. https://doi.org/10.1080/11035897.2013.862852.

Li, Q., Li, Y., Wang, J., Kiessling, W., 2015. Early Ordovician lithistid sponge–*Calathium* reefs on the Yangtze Platform and their paleoceanographic implications. Palaeogeogr. Palaeoclimatol. Palaeoecol. 425, 84–96. https://doi.org/10.1016/j.palaeo.2015.02.034.

Li, Q., Li, Y., Kiessling, W., 2017. The oldest labechiid stromatoporoids from intraskeletal crypts in lithistid sponge-*Calathium* reefs. Lethaia 50, 140–148. https://doi.org/10.1111/let.12182.

Li, Q., Agematsu, S., Na, L., Sardsud, A.A., 2019a. Stromatolite abundance anomaly in Early Ordovician: the rise of sponge-microbial association? In: Obut, O.T., Sennikov, N.V., Kipriyanova, T.P. (Eds.), 13th International Symposium on the Ordovician System, Novosibirsk, pp. 113–114.

Li, Q., Sone, M., Lehnert, O., Na, L., 2019b. Early Ordovician sponge-bearing microbialites from Peninsular Malaysia: the initial rise of metazoans in reefs. Palaeoworld 28, 80–95. https://doi.org/10.1016/j.palwor.2018.08.005.

Luo, C., 2015. "Keratose" Sponge Fossils and Microbialites: A Geobiological Contribution to the Understanding of Metazoan Origin. Ph.D Thesis, Georg-August-Universität Göttingen (151 pp).

Luo, C., Reitner, J., 2014. First report of fossil "keratose" demosponges in Phanerozoic carbonates: preservation and 3-D reconstruction. Naturwissenschaften 101, 467–477. https://doi.org/10.1007/s00114-014-1176-0.

Luo, C., Reitner, J., 2016. 'Stromatolites' built by sponges and microbes - a new type of Phanerozoic bioconstruction. Lethaia 49, 555–570. https://doi.org/10.1111/let.12166.

Meroz-Fine, E., Shefer, S., Ilan, M., 2005. Changes in morphology and physiology of an East Mediterranean sponge in different habitats. Mar. Biol. 147, 243–250. https://doi.org/10.1007/s00227-004-1532-2.

Miller, J.F., Evans, K.R., Dattilo, B.F., 2012. The Great American Carbonate Bank in the miogeocline of western central Utah: tectonic influences on sedimentation. In: Derby, J.R., Fritz, R.D., Longacre, S.A., Morgan, W.A., Sternbach, C.A. (Eds.), The Great American Carbonate Bank: The Geology and Economic Resources of the Cambrian-Ordovician Sauk Megasequence of Laurentia. AAPG Memoir 98, AAPG, pp. 769–854. https://doi.org/10.1306/13331516M983498.

Montañez, I.P., 1994. Late diagenetic dolomitization of Lower Ordovician, Upper Knox Carbonates: a record of the hydrodynamic evolution of the Southern Appalachian Basin. AAPG Bull. 78, 1210–1239. https://doi.org/10.1306/A25FEAB3-171B-11D7-8645000102C1865D.

Palumbi, S.R., 1984. Tactics of acclimation: morphological changes of sponges in an unpredictable environment. Science 225, 1478–1480. https://doi.org/10.1126/science.225.4669.1478.

Pratt, B.R., 1989. Early Ordovician cryptalgal-sponge reefs, Survey Peak Formation, Rocky Mountains, Alberta. In: Geldsetzer, H.H.J., James, N.P., Tebbutt, G.E. (Eds.), Reefs: Canada and Adjacent Areas. Canadian Society of Petroleum Geologists Memoir 13, Canadian Society of Petroleum Geologists, pp. 213–217.

Pruss, S.B., Clemente, H., Laflamme, M., 2012. Early (Series 2) Cambrian archaeocyathan reefs of southern Labrador as a locus for skeletal carbonate production. Lethaia 45, 401–410. https://doi.org/10.1111/j.1502-3931.2011.00299.x.

Reitner, J., 1993. Modern cryptic microbialite/metazoan facies from Lizard Island (Great Barrier Reef, Australia) formation and concepts. Facies 29, 3–40. https://doi.org/10.1007/BF02536915.

Riding, R., 2002. Structure and composition of organic reefs and carbonate mud mounds: concepts and categories. Earth Sci. Rev. 58, 163–231. https://doi.org/10.1016/S0012-8252(01)00089-7.

Riding, R., 2011. Microbialites, stromatolites, and thrombolites. In: Reitner, J., Thiel, V. (Eds.), Encyclopedia of Geobiology. Springer, Heidelberg, pp. 635–654. https://doi.org/10.1007/978-1-4020-9212-1_196.

Rigby, J.K., Desrochers, A., 1995. Lower and Middle Ordovician lithistid demosponges from the Mingan Islands, Gulf of St. Lawrence, Quebec, Canada. Paleontol. Soc. Mem. 41, 1–35.

Rowland, S.M., Shapiro, R.S., 2002. Reef patterns and environmental influences in the Cambrian and earliest Ordovician. In: Kiessling, W., Flügel, E., Golonka, J. (Eds.), Phanerozoic Reef Patterns. SEPM Special Publication 72, SEPM, Tulsa, pp. 95–128. https://doi.org/10.2110/pec.02.72.0095.

Sarà, M., Bavestrello, G., Cattaneo-Vietti, R., Cerrano, C., 1998. Endosymbiosis in sponges: relevance for epigenesis and evolution. Symbiosis 25, 57–70.

Shapiro, R.S., 2000. A comment on the systematic confusion of thrombolites. Palaios 15, 166–169. https://doi.org/10.1669/0883-1351(2000)015<0166:ACOTSC>2.0.CO;2.

Shapiro, R.S., Rigby, J.K., 2004. First occurrence of an *in situ* anthaspidellid sponge in a dendrolite mound (Upper Cambrian; Great Basin, USA). J. Paleontol. 78, 645–650. https://doi.org/10.1666/0022-3360(2004)078<0645:FOOAIS>2.0.CO;2.

Shen, Y., Neuweiler, F., 2018. Questioning the microbial origin of automicrite in Ordovician calathid-demosponge carbonate mounds. Sedimentology 65, 303–333. https://doi.org/10.1111/sed.12394.

Toomey, D.F., 1970. An unhurried look at a Lower Ordovician mound horizon, southern Franklin Mountains, west Texas. J. Sediment. Petrol. 40, 1318–1334. https://doi.org/10.1306/74D72194-2B21-11D7-8648000102C1865D.

Toomey, D.F., Ham, W.E., 1967. *Pulchrilamina*, a new mound-building organism from Lower Ordovician rocks of west Texas and southern Oklahoma. J. Paleontol. 41, 981–987.

Walter, M.R., 1972. Stromatolites and the biostratigraphy of the Australian Precambrian and Cambrian. In: Special Papers in Palaeontology 11. The Palaeontological Association, London (256 pp).

Webby, B.D., 2002. Patterns of Ordovician reef development. In: Kiessling, W., Flügel, E., Golonka, J. (Eds.), Phanerozoic Reef Patterns. SEPM Special Publication 72, SEPM, Tulsa, pp. 129–179. https://doi.org/10.2110/pec.02.72.0129.

Whalan, S., Webster, N.S., 2014. Sponge larval settlement cues: the role of microbial biofilms in a warming ocean. Sci. Rep. 4, 4072. https://doi.org/10.1038/srep04072.

Wilkinson, C.R., Fay, P., 1979. Nitrogen fixation in coral reef sponges with symbiotic cyanobacteria. Nature 279, 527–529. https://doi.org/10.1038/279527a0.

Wright, V.P., Cherns, L., 2016. Leaving no stone unturned: the feedback between increased biotic diversity and early diagenesis during the Ordovician. J. Geol. Soc. 173, 241–244. https://doi.org/10.1144/jgs2015-043.

Wyatt, D.J., 1979. Carbonate mud mounds from the Lower Ordovician Wah Wah Limestone of the Ibex area, western Millard County, western Utah. Brigham Young University Geology Studies 26, 101–114. https://doi.org/10.1144/jgs2015-043.

Zhao, H., Zhang, S., Zhu, M., Ding, J., Li, H., Yang, T., Wu, H., 2021. Paleomagnetic insights into the Cambrian biogeographic conundrum: did the North China craton link Laurentia and East Gondwana? Geology 49, 372–376. https://doi.org/10.1130/g47932.1.

Zhuravlev, A.Y., Naimark, E.B., Wood, R.A., 2015. Controls on the diversity and structure of earliest metazoan communities: Early Cambrian reefs from Siberia. Earth Sci. Rev. 147, 18–29. https://doi.org/10.1016/j.earscirev.2015.04.008.